Fitoterapia 138 (2019) 104294

Contents lists available at ScienceDirect

Fitoterapia

journal homepage: www.elsevier.com/locate/fitote

New eremophilane-type sesquiterpenes and maleimide-bearing compounds from *Carpesium abrotanoides* L.

Lei Wang[a,e], Guan Jin[a], Li Tian[a], Weaam Ebrahim[d], Simon-Patrick Höfert[c], Christoph Janiak[c], Jian-Feng Chen[a], Zhi-Yong Guo[a], Till F. Schäberle[e], Zhen Liu[b,*], Fan Cheng[a,*], Peter Proksch[b,*], Kun Zou[a,*]

[a] Hubei Key Laboratory of Natural Products Research and Development, College of Biological and Pharmaceutical Sciences, China Three Gorges University, Yichang 443002, China
[b] Institute of Pharmaceutical Biology and Biotechnology, Heinrich-Heine-University Duesseldorf, 40225 Duesseldorf, Germany
[c] Institute of Inorganic and Structural Chemistry, Heinrich-Heine-University Düsseldorf, 40204 Düsseldorf, Germany
[d] Department of Pharmacognosy, Faculty of Pharmacy, Mansoura University, Mansoura 35516, Egypt
[e] Institute for Insect Biotechnology, Justus-Liebig-University of Giessen, 35392 Giessen, Germany

ARTICLE INFO

Keywords:
Carpesium abrotanoides L.
Sesquiterpenes
Maleimide-bearing compounds
Cytotoxicity

ABSTRACT

Two new eremophilane-type sesquiterpenes, carperemophilanes A and B (**1**–**2**), three new maleimide-bearing compounds, carpesiumaleimides A–C (**3**–**5**), along with a known sesquiterpene, carabrol (**6**), were isolated from the ethanol extract of *Carpesium abrotanoides* L. Their structures were elucidated by analysis of their NMR and MS data as well as by comparison with the literature. The absolute configuration of carperemophilane A (**1**) was determined by single-crystal X-ray diffraction analysis. All isolated compounds (**1**–**6**) were evaluated *in vitro* for cytotoxicity against two human cancer cell lines MDA-MB-231 and HGC-27 using the MTT method. Compounds **1**, **2** and **6** showed cytotoxic activities with IC_{50} values ranging from 7.45 to 37.35 μM.

1. Introduction

Carpesium abrotanoides L. (Asteraceae) is widely distributed in China and Korea, predominantly in the mountainous areas of Southwest China. The seeds of *C. abrotanoides* have a long history of medicinal use for treating various diseases such as ascariasis, enterobiasis, cestodiasis and abdominal pain due to parasitic infections [1]. Up to now, a series of sesquiterpene lactones and dimers have been isolated from *C. abrotanoides*, some of which showed diverse biological activities including antitumor, antiplasmodial, anti-inflammatory and antibacterial effects [2–11]. In continuation of our search for new bioactive metabolites from traditional herbal medicine [12–13], two new eremophilane-type sesquiterpenes, carperemophilanes A and B (**1**–**2**), three new maleimide-bearing compounds, carpesiumaleimides A–C (**3**–**5**), together with a known sesquiterpene, carabrol (**6**), were isolated from the ethanol extract of *C. abrotanoides*. Nature products with maleimide-bearing skeleton are scarce from plants, to date, only one such compounds, named turrapubesins B, has been reported from the twigs and leaves of *Turraea pubescens* [14], suggesting that the biosynthesis of **3**–**5** may involve the contribution of endophytic fungi [15]. In this paper, the isolation, structural elucidation and cytotoxicity of these compounds are presented.

2. Results and discussion

Compound **1** was obtained as colorless crystals. The HRESIMS of **1** showed a pseudomolecular ion at *m/z* 291.1565 $[M + Na]^+$, indicating the molecular formula $C_{15}H_{24}O_4$ with four degrees of unsaturation. The ^{13}C NMR spectrum of **1** (Table 1) displayed one carbonyl carbon at δ_C 171.5 (C-12), two olefinic carbons at δ_C 149.6 (C-11) and 122.0 (C-13), two oxygenated carbons at δ_C 76.2 (C-1) and 75.5 (C-10), and two methyl groups at δ_C 18.1 (Me-14) and 15.6 (Me-15). The ^1H NMR spectrum of **1** (Table 1) exhibited two methyl groups at δ_H 0.96 (s, Me-14) and 0.69 (d, J = 6.8 Hz, Me-15), and two olefinic protons at δ_H 6.09 (s, H-13a) and 5.68 (dd, J = 1.1, 0.7 Hz, H-13b). The above spectroscopic data accounted for two degrees of unsaturation, and the remaining two degrees of unsaturation were represented by a bicyclic carbon skeleton. The COSY correlations between H-1 (δ_H 3.44)/H-2a (δ_H 2.19), H-1/H-2b (δ_H 1.49), H-2b/H-3b (δ_H 1.16), Me-15/H-4 (δ_H 1.77), H-6b (δ_H 1.59)/H-7 (δ_H 2.94), H-8a (δ_H 2.16)/H-7, H-8a/H-9a (δ_H 2.41), together with the HMBC correlations from Me-15 to C-3 (δ_C 26.5), C-4 (δ_C 36.7) and C-5 (δ_C 40.6), from Me-14 to C-4, C-5, C-6 (δ_C

* Corresponding authors.
E-mail addresses: zhenfeizi0@sina.com (Z. Liu), chengf@ctgu.edu.cn (F. Cheng), proksch@uni-duesseldorf.de (P. Proksch), kzou@ctgu.edu.cn (K. Zou).

https://doi.org/10.1016/j.fitote.2019.104294
Received 10 July 2019; Received in revised form 3 August 2019; Accepted 5 August 2019
Available online 06 August 2019
0367-326X/

Table 1
^{1}H (300 MHz) and ^{13}C NMR (75 MHz) data of compounds **1** and **2** in CD_3OD.

Position	**1**		**2**	
	δ_C	δ_H (J in Hz)	δ_C	δ_H (J in Hz)
1	76.2	3.44 dd (2.3, 1.5)	76.5	3.42 dd (3.4, 2.1)
2	29.8	2.19 m	29.8	2.21 m
		1.49 m		1.52 m
3	26.5	1.53 m	26.7	1.61 td (13.6, 4.3)
		1.16 m		1.21 m
4	36.7	1.77 m	36.1	1.86 m
5	40.6	–	40.5	–
6	38.5	1.85 dd (13.6, 7.1)	40.5	1.99 dd (13.4, 7.1)
		1.59 d (13.1)		1.47 m
7	34.2	2.94 br s	36.0	2.68 br s
8	23.4	2.16 m	23.0	2.18 m
		1.85 dd (13.6, 7.1)		1.77 d (13.5)
9	29.5	2.41 ddd (13.9, 11.8, 5.3)	28.8	2.27 m
		1.20 m		1.12 dt (12.8, 3.4)
10	75.5	–	75.0	–
11	149.6	–	158.8	7.20 dd (15.9, 5.1)
12	171.5	–	119.1	5.81 dd (15.9, 2.2)
13	122.0	6.09 s	170.7	–
		5.68 dd (1.1, 0.7)		
14	18.1	0.96 s	18.0	0.97 s
15	15.6	0.69 d (6.8)	15.6	0.74 d (6.9)

38.5) and C-10, and from H-1 to C-3, C-5, C-9 (δ_C 29.5) and C-10, established the bicyclic nucleus with two methyl substituents at C-4 and C-5 as well as two hydroxy groups at C-1 and C-2, respectively. The attachment of an allylic acid moiety at C-7 was deduced from the HMBC correlations from H-13a and H-13b to C-7 (δ_C 34.2), C-11 (δ_C 149.6) and C-12 (δ_C 171.5) (Fig. 2). Thus, the planar structure of **1** was elucidated, representing a new eremophilane-type sesquiterpene, for which the trivial name carperemophilane A is proposed.

The relative configuration of caroeremophilane A (**1**) was established on the basis of the ROESY spectrum (Fig. 3). The ROESY correlations between Me-14/H-13b, H-13b/H-9a, H-9a/Me-14, Me-14/Me-15 and between H-9b/H-1 suggested that Me-14 and Me-15 were on the same side of the ring, while H-1, H-4 and H-7 were on the opposite side. Moreover, the absolute configuration of caroeremophilane A (**1**) was determined as 1*R*, 4*S*, 5*R*, 7*S*, and 10*R* by single-crystal X-ray diffraction analysis (Fig. 4). In the solid-state packing of compound **1**, it is remarkable to note that the carboxyl group does not enter into the common head-to-tail hydrogen-bonding arrangement with the carboxyl group of an adjacent molecule. Instead, the carboxyl group donates and accepts a hydrogen bond to two different hydroxy groups of two adjacent molecules, with all three groups forming an 8-membered hydrogen-bonded ring (Fig. 4b). Thus, the structure of **1** was unambiguously elucidated as shown in Fig. 1.

Compound **2** was obtained as white amorphous powder. The molecular formula of **2** was determined as $C_{15}H_{24}O_4$ on the basis of HRESIMS data. Its NMR data (Table 1) were similar to those of **1**, suggesting an eremophilane-type skeleton for **2**. The main difference of the NMR data between them was that the signals of a methylene group at δ_C 122.0 (C-13) and a quaternary carbon at δ_C 149.6 (C-11) in **1** were replaced by two olefinic methines at δ_C 158.8 (C-11) and 119.1 (C-12) in **2**, suggesting that the terminal double bond was replaced by a 1,2-disubstituted olefin in **2**. This can be confirmed by the COSY correlations between H-12 (δ_H 5.81)/H-11 (δ_H 7.20)/H-7 (δ_H 2.68) along with the HMBC correlations from H-11 to C-8 (δ_C 23.0), C-7 (δ_C 36.0), C-6 (δ_C 40.5) and C-13 (δ_C 170.7), and from H-12 to C-7 and C-13. The C-11/C-12 double bond was shown to adopt *E* configuration based on the coupling constant (15.9 Hz). The remaining substructure of **2** was identical to **1** as evident from COSY and HMBC spectra (Fig. 2). The relative configuration of **2** was determined to be identical to that of **1** on the basis of the similar coupling constants and NOE relationships. Due to the close biogenetic relationship of compounds **1** and **2** the absolute configuration of **2** is suggested to be identical to that of **1**.

Compound **3** was obtained as colorless oil. The molecular formula of **3** was determined as $C_{13}H_{19}NO_4$ with five degrees of unsaturation. The ^{1}H NMR data of **3** (Table 2) exhibited four methyl groups at δ_H 0.92 (t, J = 7.5 Hz, Me-3′), 1.21 (d, J = 6.9 Hz, Me-4′), 1.07 (d, J = 6.7 Hz, Me-3″) and 0.84 (d, J = 6.8 Hz, Me-4″), two methylene protons at δ_H 1.69 (m, H-2'a) and δ_H 1.55 (m, H-2'b), an olefinic methine proton at δ_H 6.45 (d, J = 1.3 Hz, H-3) and three aliphatic methine protons at δ_H 2.67 (qd, J = 6.8, 1.2 Hz, H-1′), 4.30 (d, J = 8.1 Hz, H-1″) and 2.58 (m, H-2″). The above data were similar to those of 2-(3-isopropyl-2,5-dioxo-2,5-dihydropyrrol-1-yl)-3-methylbutyric acid, a synthetic maleimide-bearing compound reported in 2013 [16]. The major difference between both compounds was the presence of an additional methylene group at δ_H 1.69 (m, H-2'a) and δ_H 1.55 (m, H-2'b) in **3**, suggesting that **3** was an analog of the synthetic compound. The COSY correlations between H-1′/Me-4′, H-1'/H-2'a, H-1'/H-2'b, H-2'a/Me −3′, H-2'b/Me-3′, H-1"/H-2″, H-2″/Me-3″ and H-2″/Me-4″, together with the HMBC correlations from H-3 to C-1′ (δ_C 33.6), C-2 (δ_C 156.1), C-1 (δ_C 172.0) and C-4 (δ_C 172.0), from H-1′ to C-1, C-2 and C-3, from H-1″ to C-1, C-4 and C-5″ (δ_C 172.4), confirmed the connection between C-1″ and the maleimide nitrogen and between C-1′ and C-2. Thus, the planar structure of **3** was elucidated as shown in Fig. 1 and the trivial name carpesiumaleimide A was given for **3**.

The molecular formula of **4** was determined as $C_{14}H_{21}NO_4$ based on the HRESIMS data. The ^{1}H NMR data of **4** were close similar to those of carpesiumaleimide A (**3**) except for the appearance of an additional methylene group in **4** at δ_H 1.48 (m, H-3″a) and 1.00 (m, H-3″b). The COSY correlations between H-1″ (δ_H 4.36, d)/H-2″ (δ_H 2.41, m), H-3"a/

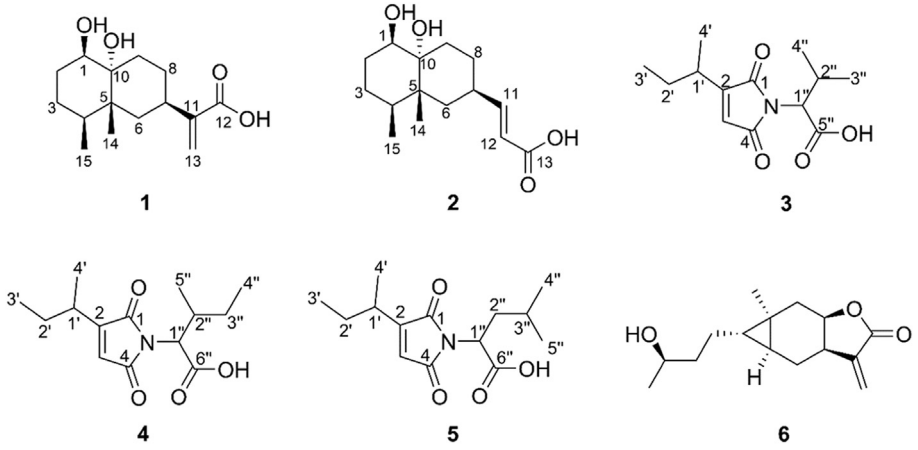

Fig. 1. Structures of compounds **1–6**.

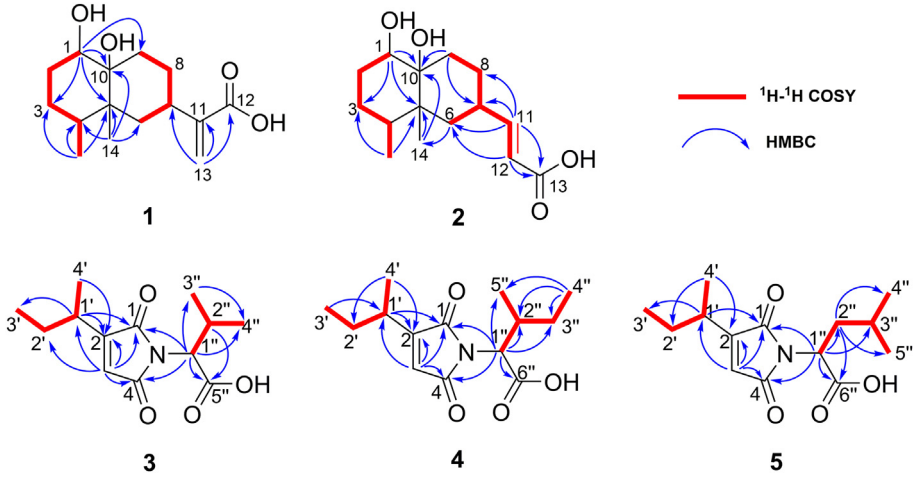

Fig. 2. The key HMBC and $^{1}H-^{1}H$ COSY correlations of compounds **1**–**5**.

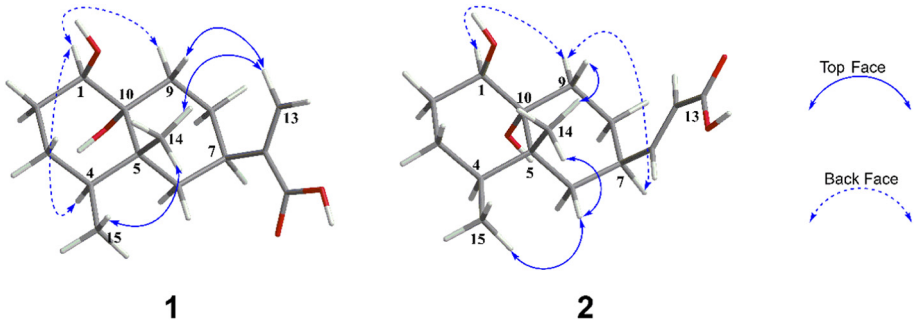

Fig. 3. The key ROESY correlations of compounds **1** and **2**.

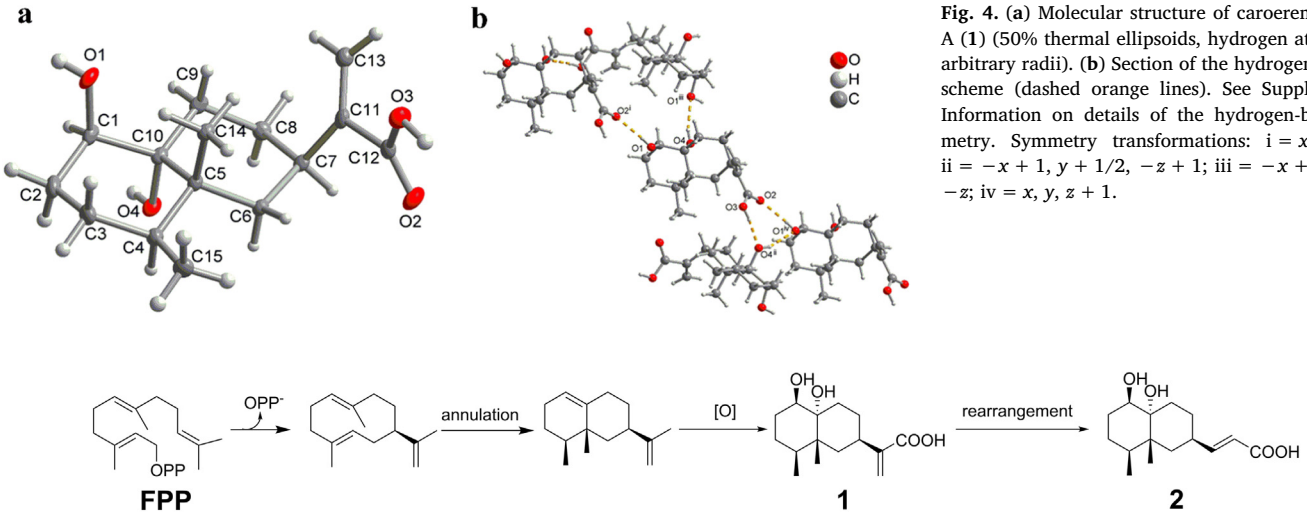

Fig. 4. (**a**) Molecular structure of caroeremophilane A (**1**) (50% thermal ellipsoids, hydrogen atoms with arbitrary radii). (**b**) Section of the hydrogen-bonding scheme (dashed orange lines). See Supplementary Information on details of the hydrogen-bond geometry. Symmetry transformations: i = *x*, *y*, *z*-1; ii = $-x+1$, $y+1/2$, $-z+1$; iii = $-x+1$, $y-1/2$, $-z$; iv = *x*, *y*, $z+1$.

Fig. 5. Plausible biogenetic pathway for compounds **1** and **2**.

H-2″, H-3”b/H-2″, Me-4″ (δ_H 0.88, t)/H-3”a, Me-4”/H-3”b and H-2″/Me-5″ (δ_H 1.07, d), together with the HMBC correlations from H-1″ to C-1 (δ_C 171.6), C-4 (δ_C 171.6) and C-6″ (δ_C 172.0) indicated the replacement of the valine residue by an isoleucine residue in **4**, when compared to **3** (Fig. 2). The remaining substructure of **4** was identical to **3** after analysis of the 2D NMR spectra of **4**.

Compound **5** shared the same molecular formula as **4**. The ^{1}H NMR data of **5** were similar to those of **4** except for the triplet signal of the methyl group which was replaced by a doublet signal in **5**. The COSY correlations between H-1″(4.48, dd)/H-2″a, H-1″/H-2″b, H-2″a/H-3″ (1.34), H-2”b/H-3″, H-3″/Me-4″ (0.82, d), H-3″/Me-5″ (0.84, d), together with the HMBC correlations from H-1″ to C-1 (δ_C 170.5), C-4 (δ_C 170.9) and C-6″ (δ_C 171.0) indicated the presence of a leucine residue in **5** instead of an isoleucine residue (Fig. 2). Thus, the structure of **5** was elucidated as shown in Fig. 1.

Compound **6** was identified as carabrol [17]. Plausible biosynthetic pathways for the isolated eremophilane-type sesquiterpenes (**1–2**) was postulated as shown in Fig. 5. From a biosynthetic point of view, the eremophilane-type sesquiterpenes are assumed to be generated by the mevalonate pathway from farnesylpyrophosphate (FPP) [18]. FPP can further transform into caroeremophilane A (**1**) by annulation and a series of oxidation. A rare rearrangement is taking place and turning an

Table 2
^{1}H NMR and ^{13}C NMR spectrum data of compounds **3–5**.

Position	3[a]		4[b,d]		5[c]	
	δ_C	δ_H (*J* in Hz)	δ_C	δ_H (*J* in Hz)	δ_C	δ_H (*J* in Hz)
1	172.0	–	171.6	–	170.5	–
2	156.1	–	155.7	–	153.4	–
3	126.7	6.45 d (1.3)	126.4	6.43 d (1.3)	126.0	6.66 d (1.1)
4	172.0	–	171.6	–	170.9	–
1′	33.6	2.67 qd (6.8, 1.2)	33.2	2.66 qd (6.8, 1.2)	31.5	2.58 qd (6.8, 0.9)
2′	29.2	1.69 m 1.55 m	28.8	1.71 m 1.57 m	27.5	1.57 m 1.47 m
3′	11.8	0.92 t (7.5)	11.4	0.94 t (7.5)	11.2	0.83 t (7.3)
4′	18.6	1.21 d (6.9)	18.2	1.22 d (6.9)	17.9	1.13 d (6.9)
1″	58.9	4.30 d (8.1)	58.3	4.36 d (8.2)	50.3	4.48 dd (11.7, 4.2)
2″	29.6	2.58 m	35.3	2.41 m	36.7	2.05 ddd (14.0, 11.9, 4.2) 1.74 ddd (14.2, 10.1, 4.3)
3″	21.4	1.07 d (6.7)	26.8	1.48 m 1.00 m	24.8	1.34 m
4″	19.8	0.84 d (6.8)	11.0	0.88 t (7.3)	20.8	0.82 d (7.3)
5″	172.4	–	17.1	1.07 d (6.7)	23.0	0.84 d (7.3)
6″	–	–	172.0	–	171.0	–

[a] Recorded in CD_3OD at 100 MHz for carbon and 400 MHz for proton.
[b] Recorded in CD_3OD at 75 MHz for carbon and 300 MHz for proton.
[c] Recorded in DMSO-d_6 at 100 MHz for carbon and 400 MHz for proton.
[d] The ^{13}C NMR data were extracted from HSQC and HMBC.

isopropyl into a n-propyl, led the apparence of caroeremophilane B (**2**).

All isolated compounds (**1–6**) were evaluated *in vitro* for cytotoxicity against two human cancer cell lines MDA-MB-231 and HGC-27 using the MTT method. Their IC_{50} values were given in Table 3. Compound **6** showed the best cytotoxicity against MDA-MB-231 and HGC-27 cancer cell lines with IC_{50} values of 7.45 and 10.27 μM, respectively.

Data are expressed as mean ± SD (n = 3).

3. Experimental

3.1. General experimental procedures

The optical rotations were measured with a JASCO P-2000 polarimeter. 1D and 2D NMR spectra were recorded using Bruker ARX 300 or Bruker AVANCE 400 MHz instruments with TMS as the intestinal standard. ESI-mass spectra were obtained using an LC-MS HP1100 Agilent Finnigan LCQ Deca XP Thermoquestman spectrometer, and HRESIMS were measured on an UHR-QTOF maXis 4G (Bruker Daltonics) mass spectrometer or a Finnigan-MAT LCQ DECA XP plus mass spectrometer. Dionex UltiMate-3400SD system coupled to an LPG-3400SD pump and a photodiode array detector (DAD 300RS) was used for HPLC analysis. The analytical column (125 × 4 mm) employed was prefilled with Eurosphere-10 C_{18} (Knauer, Germany), and the following gradient was used (MeOH, 0.1% formic acid in H_2O): 0 min (10% MeOH); 5 min (10% MeOH); 35 min (100% MeOH); 45 min (100% MeOH). The Semi-preparative HPLC was performed using a Merck Hitachi HPLC System (UV detector L-7400; pump L-7100; Eurosphere-100 C_{18}, 300 × 8 mm), with a mixture of MeOH and H_2O as mobile phases. Column chromatography utilized Merck MN silica gel 60 M (0.04–0.063 mm). TLC plates precoated with silica gel F254 (Merck) were used to monitor and collect fractions with detection under 254 and 366 nm or by spraying the plates with anisaldehyde reagent. Distilled and spectroscopic grade solvents were used for column chromatography and spectroscopic measurements, respectively. Optical density (OD) values for the 3-(4,5-dimethylthiazol-2-yl)-2,5-diphenyltetrazolium bromide (MTT) assays were read on automated microplate reader (ELX 800, France). Pre-distilled and spectroscopic grade solvents were used for both column chromatography and spectroscopic measurements, respectively.

Table 3
Cytotoxic activities of compounds **1–6**.

Compound	IC_{50} (μM)	
	MDA-MB-231	HGC-27
1	22.67 ± 0.66	24.83 ± 0.96
2	34.83 ± 1.16	37.35 ± 0.76
3	> 50	> 50
4	> 50	> 50
5	> 50	> 50
6	7.45 ± 0.48	10.27 ± 0.55
mitomycin C	4.89 ± 0.81	6.73 ± 0.92

3.2. Plant material

In July 2015, the whole plants of *C. abrotanoides* were collected at Changyang, Hubei Province, People's Republic of China, and identified by Dr. Yu-Bing Wang. A voucher specimen (No. 2015072701) was deposited at Hubei Key Laboratory of Natural Products Research and Development, China Three Gorges University.

3.3. Extraction and isolation

The whole plants (7.5 kg) were air-dried, powdered and then followed by extraction with 95% EtOH (15 L × 3) under reflux. The EtOH extract (504 g) was obtained after removal of solvent *in vacuo* and freeze-drying. The extract was then suspended in water (1.5 L), and then extracted with petroleum ether, EtOAc and n-BuOH, respectively. The EtOAc extract (161 g) was fractionated by silica gel column chromatography (2300 g, 200–300 mesh) and eluted with a gradient of $CHCl_3$/MeOH (*v*/v, 100% $CHCl_3$ to100% MeOH) to obtain 15 fractions (Fr. 1–15). Fr. 10 (16.8 g) was further separated by vacuum liquid chromatography on a silica gel column (80 × 300 mm) eluted with a gradient of *n*-hexane and EtOAc (from 9:1 to 1:2) to give eleven subfractions (Fr. 10.1–10.11), Fr. 10.8 (1.1 g) was subjected to a Sephadex LH-20 column (60 × 3 cm) with MeOH as mobile phase to remove pigments, and then purified by semipreparative HPLC (MeOH-H_2O: 0–5 min, 35%; 5–18 min, from 35% to 60%; 19–25 min, 100%) to give **1** (5.1 mg). Following the same protocol, compound **2** (4.6 mg) was obtained from Fr. 10.9 (0.9 g) (HPLC sequence, MeOH-H_2O: 0–8 min, from 20% to 45%; 8–22 min, from 45% to 70%; 22–30 min, 100%). Fr. 9 (9.7 g) was further separated by vacuum liquid chromatography on a Silica gel column (80 × 300 mm) eluted with a gradient of CH_2Cl_2 and MeOH (from 9:1 to 1:9) to give nine subfractions (Fr. 9.1–9.9), Fr. 9.6 (1.4 g) was subjected to a Sephadex LH-20 column (60 × 3 cm) with MeOH as mobile phase to remove pigments, and then purified by semipreparative HPLC (MeOH-H_2O: 0–9 min, 28%; 9–25 min, from 28% to 55%; 25–30 min, 100%) to give **3** (1.3 mg), **4** (1.1 mg) and **5** (0.9 mg).

*Carperemophilane A (**1**)*: colorless crystals; $[\alpha]_D^{20}$ −53 (c = 0.51; CH_3OH); UV (MeOH) λ_{max} 215 nm; ^{1}H NMR (CD_3OD, 300 MHz) and ^{13}C NMR (CD_3OD, 75 MHz) data see Table 1; HRESIMS *m/z* 291.1565 $[M + Na]^+$ (calcd. For $C_{15}H_{24}O_4Na$, 291.1572).

*Carperemophilane B (**2**)*: white amorphous powder; $[\alpha]_D^{20}$ −24 (c = 0.14; CH_3OH); UV (MeOH) λ_{max} 232 nm; ^{1}H NMR (CD_3OD, 300 MHz) and ^{13}C NMR (CD_3OD, 75 MHz) data see Table 1; HRESIMS *m/z* 291.1572 $[M + Na]^+$ (calcd. For $C_{15}H_{24}O_4Na$, 291.1572).

*Carpesiumaleimide A (**3**)*: colorless oil; $[\alpha]_D^{20}$ −13.9 (c = 0.47; CH_3OH); UV (MeOH) λ_{max} 227 nm; ^{1}H NMR (CD_3OD, 400 MHz) and ^{13}C NMR (CD_3OD, 100 MHz) data see Table 2; HRESIMS *m/z* 276.1205 $[M + Na]^+$ (calcd. For $C_{13}H_{19}NO_4Na$, 276.1212).

*Carpesiumaleimide B (**4**)*: colorless oil; $[\alpha]_D^{20}$ −22.1 (c = 0.85; CH_3OH); UV (MeOH) λ_{max} 228 nm; ^{1}H NMR (CD_3OD, 300 MHz) and

^{13}C NMR (CD_3OD, 75 MHz) data see Table 2; HRESIMS *m/z* 290.1364 $[M + Na]^+$ (calcd. For $C_{13}H_{19}NO_4Na$, 290.1368).

Carpesiumaleimide C (***5***): colorless oil; $[\alpha]_D^{20} - 31.6$ (c = 0.69; CH_3OH); UV (MeOH) λ_{max} 226 nm; ^{1}H NMR (DMSO-d_6, 400 MHz) and ^{13}C NMR (DMSO-d_6, 100 MHz) data see Table 2; HRESIMS *m/z* 290.1364 $[M + Na]^+$ (calcd. For $C_{13}H_{19}NO_4Na$, 290.1368).

3.4. X-ray crystallographic analysis of compound *1*

Crystallization conditions: Slow evaporation of a MeOH solution containing compound **1** was employed in order to obtain X-ray quality crystals of **1**. A suitable single crystal was carefully picked under a polarizing microscope. Data collection: The crystal structure of compound **1** was measured using Cu-Kα radiation (λ = 1.54178 Å) on a Bruker Kappa APEX2 CCD diffractometer with a microfocus tube. Data collection was carried out using the program APEX2 [19], cell refinement and data reduction using SAINT [19], and experimental absorption correction using SADABS [20]. The structure was solved by intrinsic phasing in SHELXT [21] and refined by full-matrix least-squares on F^2 in SHELXL-2017 [22]. Carbon bonded hydrogen atoms were positioned geometrically (C-H = 1.00 Å for tertiary C—H, 0.99 Å for CH_2 and 0.98 Å for CH_3). Riding models (AFIX 13, 23, 137) were used for refinement with $U_{iso}(H) = 1.2\ U_{eq}$ (CH, CH_2) and $1.5\ U_{eq}$ (CH_3). The Hydrogen atoms for OH were positioned and refined freely with $U_{iso}(H) = 1.5\ U_{eq}(O)$.

The absolute structure of **1** was determined by anomalous dispersion from Cu-Kα radiation. The resulting Flack parameter of x = 0.13 [4] is close to zero, confirming the absolute structure [23–24]. Due to low Friedel pair coverage a bayesian statistics analysis of Bijvoet pair differences was necessary [25]. The drawing of all graphics was done in DIAMOND [26]. The analyses of hydrogen bonds and CH-π interactions was done in PLATON for Windows [27–30].The structure has been deposited in the Cambridge Crystallographic Data Centre (CCDC No. 1910139).

Crystal Data of **1**: $C_{15}H_{24}O_4$, M = 268.34, monoclinic system, space group $P2_1$, a = 6.9108 [7] Å, b = 10.1955 [10] Å, c = 10.0716 [10] Å, V = 678.50 [12] Å^3, Z = 2, D_{calc} = 1.313 g/cm^3, crystal size 0.25 × 0.25 × 0.13 mm, μ(Cu Ka) = 0.76 mm^{-1}, 4.6° < θ < 65.8°, N_t = 8006, N = 2191 (R_{int} = 0.024), R_1 = 0.024, wR_2 = 0.063, S = 1.10, Flack parameter x = 0.13 [4], Hooft parameter = 0.11 [3], probability for correct absolute structure $P2$(true) = 1.000, probability for wrong absolute structure $P3$(false) = $0.9 \cdot 10^{-150}$.

3.5. Cytotoxicity assay

Cytotoxicity assays against the MDA-MB-231 human breast cancer cell line and the HGC-27 human gastric cancer cell line were performed according to the MTT method as described previously [31]. Mitomycin C was used as positive control and medium with 0.1% DMSO was used as negative control.

Acknowledgements

This research was financially supported by grants from the National Natural Science Foundations of China (No. 81773952, 21272136 and 21272137), and the Opening Foundation of the State Key Laboratory of Mycology (SKLMKF201501), and the Startup Foundation of China Three Gorges University. P.P. wants to thank the Manchot Foundation for support.

Declaration of Competing of Interest

We declare that none of the authors have any financial or scientific conflicts of interest with regard to the research described in this manuscript.

Appendix A. Supplementary data

Supplementary data to this article can be found online at https://doi.org/10.1016/j.fitote.2019.104294.

References

[1] Editorial Committee of the Chinese Academy of Science, Flora of China, 75 Science Press, Beijing, 1979, p. 313.
[2] H.B. Wu, H.B. Wu, W.S. Wang, T.T. Liu, M.G. Qi, J.C. Feng, X.Y. Li, Y. Liu, Insecticidal activity of sesquiterpene lactones and monoterpenoid from the fruits of *Carpesium abrotanoides* L, Ind. Crops Prod. 92 (2016) 77–83.
[3] M. Maruyama, A. Karube, K. Sato, Sesquiterpene lactones from *Carpesium abrotanoides* L, Phytochemistry 22 (1983) 2773–2774.
[4] F. Wang, K. Yang, F.C. Ren, J.K. Liu, Sesquiterpene lactones from *Carpesium abrotanoides* L, Fitoterapia 80 (2009) 21–24.
[5] J. Wu, C. Tang, L. Chen, Y. Qiao, M. Geng, Y. Ye, Dicarabrones A and B, a pair of new epimers dimerized from sesquiterpene lactones via a [3 + 2] cycloaddition from *Carpesium abrotanoides* L, Org. Lett. 17 (2015) 1656–1659.
[6] J.F. Wang, W.J. He, X.X. Zhang, B.Q. Zhao, Y.H. Liu, X.J. Zhou, Dicarabrol, a new dimeric sesquiterpene from *Carpesium abrotanoides* L, Bioorg. Med. Chem. Lett. 25 (2015) 4082–4084.
[7] J.W. Wu, C. Tang, C.Q. Ke, S. Yao, H.C. Liu, L.G. Lin, Y. Ye, Dicarabrol A, dicarabrone C and dipulchellin A, unique sesquiterpene lactone dimers from *Carpesium abrotanoides* L, RSC Adv. (8) (2017) 4639–4644.
[8] J. Lee, B. Min, S. Lee, M. Na, B. Kwon, C. Lee, Y. Kim, K. Bae, Cytotoxic sesquiterpene lactones from *Carpesium abrotanoides* L, Planta Med. 68 (2002) 745–747.
[9] J.J. Kim, I.M. Chung, J.C. Jung, M.Y. Kim, H.I. Moon, *In vivo* antiplasmodial activity of 11(13)-dehydroivaxillin from *Carpesium cernuum*, J. Enzyme Inhib. Med. Chem. 24 (2009) 247–250.
[10] C. Yang, Y.P. Shi, Z.J. Jia, Sesquiterpene lactone glycosides, eudesmanolides, and other constituents from *Carpesium macrocephalum*, Planta Med. 68 (2002) 626–630.
[11] H.J. Lee, H.J. Lim, D.Y. Lee, H. Jung, M.R. Kim, D.C. Moon, K.I. Kim, M.S. Lee, J.H. Ryu, Carabrol suppresses LPS-induced nitric oxide synthase expression by inactivation of p38 and JNK via inhibition of I-κBα degradation in RAW 264.7 cells, Biochem. Biophys. Res. Commun. 391 (2010) 1400–1404.
[12] L. Wang, W. Qin, L. Tian, X.X. Zhang, F. Lin, F. Cheng, J.F. Chen, C.X. Liu, Z.Y. Guo, P. Proksch, K. Zou, Caroguaianolide A–E, five new cytotoxic sesquiterpene lactones from *Carpesium abrotanoides* L, Fitoterapia 127 (2018) 349–355.
[13] L. Tian, F. Cheng, L. Wang, W. Qin, K. Zou, J.F. Chen, CLE-10 from *Carpesium abrotanoides* L. suppresses the growth of human breast cancer cells (MDA-MB-231) in vitro by inducing apoptosis and pro-death autophagy via the PI3K/Akt/mTOR signaling pathway, Molecules 24 (2019) 1091.
[14] X.N. Wang, S. Yin, C.Q. Fan, F.D. Wang, L.P. Lin, J. Ding, J.M. Yue, Turrapubesins A and B, first examples of halogenated and maleimide-bearing limonoids in nature from *Turraea pubescens*, Org. Lett. 8 (2006) 3845–3848.
[15] A.A.L. Gunatilaka, Natural products from plant-associated microorganisms: distribution, structural diversity, bioactivity, and implications of their occurrence, J. Nat. Prod. 69 (2006) 509–526.
[16] S.T. Aiwale, P. Sardi, S. Dallavalle, Improved synthesis of farinomalein and its analogs, Synthetic Commun. 43 (2013) 1455–1459.
[17] M. Maruyama, A. Karube, K. Sato, Sesquiterpene lactones from *Carpesium abrotanoides*, Phytochemistry 22 (1983) 2773–2774.
[18] S.W. Niu, D. Liu, Z.Z. Shao, P. Proksch, W.H. Lin, Eremophilane-type sesquiterpenoids in a deep-sea fungus *Eutypella* sp. activated by chemical epigenetic manipulation, Tetrahedron 74 (2018) 7310–7325.
[19] Apex2, Data Collection Program for the CCD Area-Detector System; SAINT, Data Reduction and Frame Integration Program for the CCD Area-Detector System, Bruker Analytical X-Ray Systems, Madison, WI, USA, 1997 – 2012.
[20] G.M. Sheldrick, SADABS: Area-Detector Absorption Correction, University of Goettingen, Germany, 1996.
[21] G.M. Sheldrick, SHELXT - integrated space-group and crystal-structure determination, Acta Crystallogr., Sect. A 71 (2015) 3–8.
[22] G.M. Sheldrick, Crystal structure refinement with SHELXL, Acta Crystallogr., Secti. C 71 (2015) 3–8.
[23] H.D. Flack, G. Bernardinelli, Absolute structure and absolute configuration, Acta Crystallogr., Sect. A 55 (1999) 908–915.
[24] H.D. Flack, On enantiomorph-polarity estimation, Acta Crystallogr., Sect. A 39 (1983) 876–881.
[25] R.W.W. Hooft, L.H. Straver, A.L. Spek, Determination of absolute structure using Bayesian statistics on Bijvoet differences, J. Appl. Crystallogr. 41 (2008) 96–103.
[26] K. Brandenburg, Diamond (Version 3.2), Crystal and Molecular Structure Visualization, Bonn, Germany (2009).
[27] A.L. Spek, Structure validation in chemical crystallography, Acta Crystallogr. Sect. D 65 (2009) 148–155.
[28] A.L. Spek, Single-crystal structure validation with the program PLATON, J. Appl. Crystallogr. 36 (2003) 7–13.
[29] A.L. Spek, Platon - A Multipurpose Crystallographic Tool, Utrecht University, Utrecht, The Netherlands, 2008.
[30] L.J. Farrugia, Windows Implementation, Version 40608, University of Glasgow, Scotland, 2008.
[31] H.Q. Zhang, Z.S. Deng, Z.Y. Guo, X. Tu, J.Z. Wang, K. Zou, Pestalafuranones F–J, five new furanone analogues from the endophytic fungus *Nigrospora* sp. BM-2, Molecules 19 (2014) 819–825.